

Growth and Excitation of Electrohydrodynamic Surface Waves

JOSEPH M. CROWLEY

Department of Electrical Engineering, Massachusetts Institute of Technology, Cambridge, Massachusetts
(Received 30 March 1965)

Waves on the surface of a capillary liquid jet stressed by a steady applied electric field will grow in space if the velocity of the jet is supercapillary. Experimental measurements of this growth rate confirm previous theoretical discussions. The excitation of these waves by means of an applied electric field with steady and time varying components is also studied theoretically, and the frequency response is found to depend on both the shape of the electrodes and on the convective growth of the waves due to the steady component of the field. The predictions of this theory are confirmed by measurements on a water jet.

INTRODUCTION

THE last few years have seen a resurgence of interest in surface electrohydrodynamics,^{1,2} a field first investigated in the last century.³ Much of this work has been concerned with the nature of linear waves on liquid surfaces stressed by electric fields, but little has been done on the methods of exciting these surface waves. In this paper, we study a method of exciting waves on the surface of a liquid jet by means of electric fields and describe several experiments designed to test the theoretical predictions of exciter performance.

To gain familiarity with the nature of the problem, we will first consider a wave propagating on the surface of a jet stressed by a constant applied electric field. Methods of exciting these waves by means of time varying applied electric fields will then be treated in varying degrees of complexity. The simplest approach neglects the disturbance of the jet due to the excitation and concerns itself only with the net change in momentum imparted to the jet by the exciting field. This is justified by the good approximation it gives to the results of both the experiments and a more detailed theoretical approach which considers the effects of small disturbances on the exciter response. Experiments are carried out to measure the growth rate of the surface waves as well as the response of the exciter. Both of these measurements are in close agreement with the theoretical predictions.

I. GROWING WAVES

A. Planar Jet

Consider a planar perfectly conducting liquid jet of thickness Δ , density ρ , and surface tension T ,

¹ J. R. Melcher, *Field Coupled Surface Waves* (The Massachusetts Institute of Technology Press, Cambridge, Massachusetts, 1963).

² N. K. Nayyar and G. S. Murty, *Proc. Phys. Soc. (London)* 75, 369 (1960).

³ J. W. S. Rayleigh, *The Theory of Sound* (Dover Publications, Inc., New York, 1953), Vol. II.

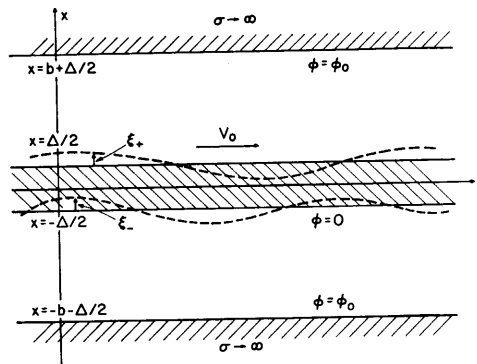


FIG. 1. The planar jet streaming to the right between parallel high voltage electrodes.

unbounded in the y and z directions and moving with a constant velocity V_0 in the z direction, as shown in Fig. 1. A constant voltage ϕ_0 is applied to two flat electrodes parallel to the undisturbed surfaces of the jet and separated from them by a distance b . The entire system, which is uniform in the y direction, is subject to a disturbance in which both sides of the jet move together (the antisymmetric mode).⁴

Although the problem contains both electric fields and a flowing fluid, its description is simplified by the fact that the electric and fluid flow fields are coupled only at the surface of the jet, making it unnecessary to solve for both fields simultaneously. By treating them separately, the form of each may be determined, and the arbitrary constants in the solution obtained by matching the boundary conditions at the surface of the jet.

The free-space region which contains the electric field is described by Maxwell's equations. In this case the interaction is quasi-static, so that the magnetic field is negligibly small. Moreover, because the fluid is highly conducting, all the charges relax to

⁴ G. Taylor, *Proc. Roy. Soc. (London)* A253, 289 (1959).

the surface. The equations then take the form

$$\nabla \cdot \mathbf{E} = 0, \quad (1a)$$

$$\nabla \times \mathbf{E} = 0, \quad (1b)$$

which implies that the electric field is the gradient of some potential function. The boundary conditions on the electric field require that the perfectly conducting surfaces of the electrodes and the jet be equipotentials.

The jet is described by the usual equations of motion for a nonviscous fluid, which are

$$\rho \, d\mathbf{v}/dt = -\nabla p, \quad (2a)$$

$$\nabla \cdot \mathbf{v} = 0, \quad (2b)$$

in the bulk. The boundary conditions at the upper and lower surfaces of the jet, including the additional effects of surface tension and electric pressure, are

$$n_i [p \delta_{ij} + \tau_{ij} - \delta_{ij} T/R_{\pm}]|_{z=\pm\Delta/2} + \xi = 0, \quad (3a, b)$$

where τ_{ij} is the Maxwell stress tensor

$$\tau_{ij} = \epsilon_0 E_i E_j - \frac{1}{2} \epsilon_0 |\mathbf{E}|^2 \delta_{ij},$$

R_{\pm} are the radii of curvature for the jet surfaces, and \mathbf{n} is the unit normal pointing out of the fluid.

To complete the specification of the problem, we must define the surface geometry and the surface normal. The surface is defined by its displacement in terms of position and time.

$$F(x, z, t) = x - \xi(z, t) = 0, \quad (4)$$

and the surface normal is given by

$$\mathbf{n} = \nabla F / |\nabla F|. \quad (5)$$

The fluid equations, linearized about the steady state operating point

$$p = \text{const}, \quad \mathbf{v} = V_0 \mathbf{i}_z,$$

are

$$\rho \left(\frac{\partial \mathbf{v}'}{\partial t} + V_0 \frac{\partial \mathbf{v}'}{\partial z} \right) = -\nabla p', \quad (6a)$$

$$\nabla \cdot \mathbf{v}' = 0, \quad (6b)$$

where the primes designate perturbation quantities. The basic solutions of these equations are waves propagating in the z direction of the form

$$f'(x, z, t) = \text{Re} [f(x) \exp i(\omega t - kz)], \quad (7)$$

with the complex amplitudes

$$\hat{p} = -(i\rho/k)(\omega - kV_0)A \sinh kx, \quad (8)$$

$$\hat{v}_x = A \cosh kx, \quad (9a)$$

$$\hat{v}_z = -iA \sinh kx, \quad (9b)$$

where the constant A is determined by the excitation. The upper and lower surfaces of the jet are defined by the equations

$$F = x \mp \frac{1}{2}\Delta - \xi'(z, t) = 0, \quad (10a, b)$$

respectively. Then, because

$$v'_z|_{z=\pm\Delta/2} = \frac{\partial \xi'}{\partial t} + V_0 \frac{\partial \xi'}{\partial z} \quad (11)$$

and from the definition of the surface normal

$$n_x = 1, \quad (12a)$$

$$n_z = -\partial \xi' / \partial z, \quad (12b)$$

the perturbed position of the surface is given as

$$\xi = -i(\omega - kV_0)^{-1} A \cosh(\frac{1}{2}k\Delta) \quad (13)$$

for both the upper and lower surfaces of the jet.

Now that an expression for the surface of the jet has been formulated in terms of the solution of the fluid mechanical equations of the system, it is possible to find the electric field in the free-space regions above and below the jet. From the boundary conditions,

$$\phi = \phi_0 \quad \text{at} \quad x = \pm(b + \frac{1}{2}\Delta), \quad (14a)$$

$$\phi = 0 \quad \text{at} \quad x = \pm\frac{1}{2}\Delta + \xi, \quad (14b)$$

the steady-state electric field is

$$E_x = \pm\phi_0/b \quad (15a, b)$$

in the upper and lower region, respectively, and the perturbed electric field is

$$\hat{e}_x = kE_0 \hat{\xi} \cosh k(b + \frac{1}{2}\Delta - x) / \sinh kb, \quad (16a)$$

$$\hat{e}_z = ikE_0 \hat{\xi} \sinh k(b + \frac{1}{2}\Delta - x) / \sinh kb. \quad (16b)$$

Substitution of these solutions into the boundary conditions on stress at the upper and lower surfaces yields the dispersion relation

$$(\omega - kV_0)^2 = \frac{Tk^3}{\rho} \coth(\frac{1}{2}k\Delta) - \frac{\epsilon_0 E_0^2 k^2}{\rho} \coth kb \coth(\frac{1}{2}k\Delta). \quad (17)$$

B. Circular Jet

These waves on the planar jet correspond to similar disturbances on a circular jet, and since experiments can be most easily performed on a circular jet, we will present the dispersion relation for this system. Consider a circular jet of radius R concentric with a larger, perfectly conducting cylinder of radius d held at the constant potential ϕ_0

measurements the imaginary part of the propagation constant was calculated. The result of one of these tests under the conditions

$$\begin{aligned} R &= 1.59 \times 10^{-3} \text{ m}, & T &= 7.2 \times 10^{-2} \text{ kg/sec}^2, \\ d &= 3.52 \times 10^{-2} \text{ m}, & \rho &= 10^3 \text{ kg/m}^3, \\ V_0 &= 5.65 \text{ m/sec}, & \phi_0 &= 13.8 \text{ kV}, \end{aligned}$$

is shown in Fig. 4. The agreement between the experimentally measured points and the curve predicted from the theory is as good as the experimental errors involved.

II. EXCITATION

A practical problem which must be faced in the study of electrohydrodynamic surface waves is excitation. These waves are electromechanical and can be excited by either electrical or mechanical means. In the work described here, all waves are excited by a force produced by an alternating electric field superposed on a steady field. If the velocity of the jet is greater than the wave velocity, the disturbances excited by this force will be swept downstream.

The physical arrangement of the system is shown in Fig. 5. The exciter is modeled by two infinitely wide, perfectly conducting parallel plates of length l on either side of the infinitely wide planar jet. The plates are separated from the grounded fluid by distances h_1 and h_2 , and potentials $\phi_{01} + e_1(t)$ and $\phi_{02} - e_2(t)$ are applied to the plates. The electric force per unit area transverse to the jet can be found by means of the relation

$$F_i = \oint \tau_{ij} n_j dA \quad (19)$$

and is

$$\begin{aligned} F_z &= \frac{1}{2} \epsilon_0 [(\phi_{01}^2/h_1^2 - \phi_{02}^2/h_2^2) \\ &\quad + 2(\phi_{01}e_1/h_1^2 + \phi_{02}e_2/h_2^2) \\ &\quad + (e_1^2/h_1^2 - e_2^2/h_2^2)]. \end{aligned} \quad (20)$$

If the relation

$$\phi_{01}/h_1 = \phi_{02}/h_2$$

is satisfied, the electric field will exert no net force on the jet in the absence of a signal voltage, and if the relation

$$e_1/h_1 = e_2/h_2$$

is satisfied, the force will be linearly proportional to the signal voltage. These conditions can be satisfied by requiring that

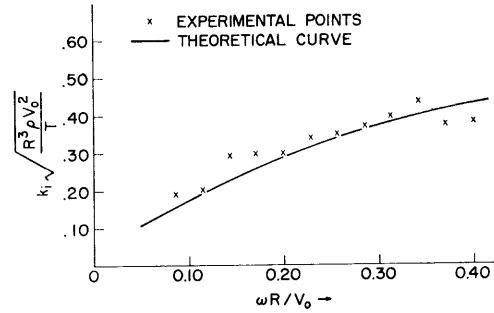


FIG. 4. Experimental and theoretical growth constant of the electrohydrodynamic surface wave as a function of frequency.

$$e_1 = e_2 = e(t), \quad h_1 = h_2 = h, \quad \phi_{01} = \phi_{02} = \phi_0,$$

so that the net force per unit area on the jet will be

$$F(t) = 2\epsilon_0 \phi_0 e(t)/h^2. \quad (21)$$

A. The Long Wavelength Limit

In the interest of simplicity, we will consider the long wavelength limit. In this special case, both the thickness of the jet and the distance between the grounded jet and the high voltage electrodes are small compared to the wavelength of disturbances on the jet. It is these assumptions which give rise to the term "long wavelength limit", and they enable the analysis of the jet to be carried out on a quasi-one-dimensional basis.

Consider a differential length of the system. The forces acting on this length will be due to the surface tension of the jet and to the electric field between the jet and the electrodes. The total force per unit area on the jet due to surface tension will be proportional to the total length of exposed surface edges, the surface tension coefficient T , and the curvature of the jet;

$$F_i = 2T \partial^2 \xi / \partial z^2. \quad (22)$$

The factor of 2 occurs because the jet has two surfaces. The net electrical force per unit area on the

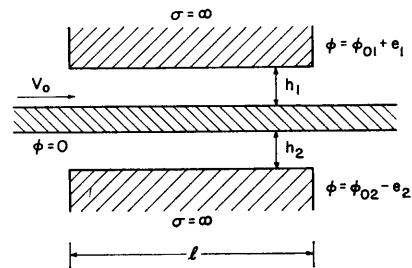


FIG. 5. The planar jet flowing through the uniform field exciter.

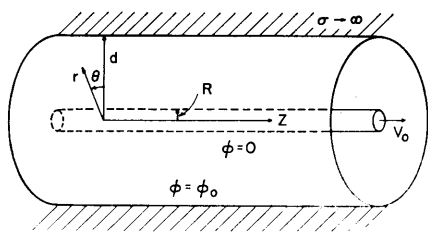


FIG. 2. Grounded circular jet streaming through a coaxial high voltage electrode.

as shown in Fig. 2. In this case, the perturbation contains a factor of the form $e^{im\theta}$ which expresses the θ dependence of the solution. The condition of periodicity in the θ direction requires that m assume only integral values, $m = 0, 1, 2, \dots$ which shows that the disturbance consists of an infinite number of circular modes. The dispersion relation for the m th mode is given by

$$(\omega - kV_0)^2 = \frac{T}{\rho R^3} \left[\frac{1}{K_m(kR)} \right] \cdot \{ \Gamma[1 + S_m(kR, kd)] - (1 - m^2) + (kR)^2 \}, \quad (18)$$

where

$$K_m(kR) = \frac{J_m(ikR)}{(ikR)J'_m(ikR)},$$

$S_m(kR, kd)$

$$= ikR \left[\frac{H'_m(ikR)J_m(ikd) - H_m(ikd)J'_m(ikR)}{H_m(ikR)J_m(ikd) - J_m(ikR)H_m(ikd)} \right],$$

$$\Gamma = \epsilon_0 \phi_0^2 / RT [\ln(d/R)]^2.$$

Here J_m is the Bessel function of the first kind, and H_m is the Hankel function of the first kind.

These dispersion relations have been thoroughly discussed elsewhere¹ and will not be treated here to any great length. It is sufficient to note that for certain real values of frequency the propagation constant k will have complex values with positive imaginary parts, which in this case indicates a wave growing in space. With an electric field applied to the jet, this growth occurs for all frequencies less than some cutoff frequency if the jet is flowing faster than the capillary velocity of the surface waves.

C. Experimental Results

Although the cutoff frequency has been measured as a function of the applied electric field in Ref. 1, no measurements of the magnitude of the growth constant, k_i , have been carried out. In order to measure this quantity, the experiment shown in Fig. 3 was performed.

A jet of tap water issues from a circular nozzle beneath a constant head of water maintained by an overflow system. The velocity of the jet at the nozzle is in the range 2–5 m/sec. After leaving the nozzle, the jet passes through the exciter, falls a distance on the order of one meter, and then flows into a mesh of wire screening, where it is brought to a stop without splashing. (Any splashing of the jet will set up vibrations on the apparatus which can be communicated back to the exciter, nozzle, and overflow tank. This feedback path results in breakup of the jet and hinders accurate measurement.)

For the derivation of the theory presented here, we must assume that the velocity of the jet is constant, an assumption which is obviously untrue for a jet falling in a gravitational field. As the jet falls, its velocity increases, and from the conservation of mass, its radius must decrease. Both of these effects will influence the growth rate of the waves. The theoretical predictions for all the experimental work were calculated for the average conditions of the region under consideration.

In this experiment, the region downstream of the exciter was surrounded by a cylindrical glass electrode with a conducting coating maintained at a constant high voltage. Spherical electrodes were used for the exciter in order to set up a nonuniform electric field and thus obtain a smooth exciter response curve, as discussed in Sec. II. Photographs of the jet were taken with the aid of a strobrotachometer and the amplitude of the waves measured as a function of distance along the jet. From these

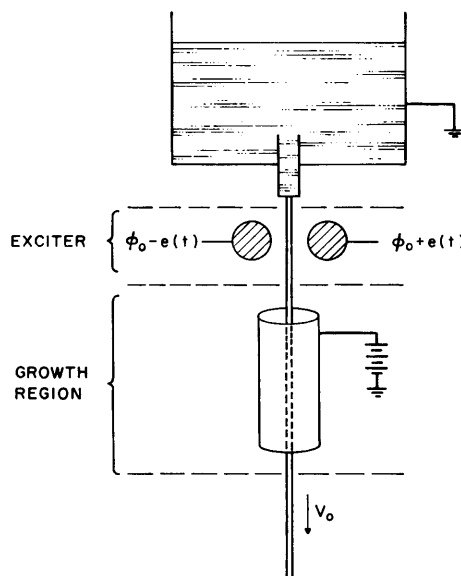


FIG. 3. Experimental apparatus, showing the reservoir, exciter, and growth region.

jet, found by integrating the Maxwell stress tensor over the surface, is

$$F_e = (2\epsilon_0\phi_0^2/h^2)[\xi/h + e(t)/\phi_0]. \quad (23)$$

Now apply Newton's law to the differential length to obtain the equation of motion of the jet

$$\left(\frac{\partial}{\partial t} + V_0 \frac{\partial}{\partial z}\right)^2 \xi = \frac{2T}{\rho\Delta} \frac{\partial^2 \xi}{\partial z^2} + \frac{2\epsilon_0\phi_0^2}{\rho\Delta h^3} \xi + \frac{2\epsilon_0\phi_0 e(t)}{\rho\Delta h^2}. \quad (24)$$

If the time-varying voltage is

$$e(t) = \text{Re} [e_0 e^{i\omega t}],$$

then the displacement can be expressed as

$$\xi = \text{Re} [\hat{\xi}(z) e^{i\omega t}],$$

and Eq. (24) becomes

$$(\rho\Delta V_0^2 - 2T) \frac{d^2 \hat{\xi}}{dz^2} + 2i\rho\Delta V_0\omega \frac{d\hat{\xi}}{dz} - \left(\rho\Delta\omega^2 + \frac{2\epsilon_0\phi_0^2}{h^3}\right) \hat{\xi} = \frac{2\epsilon_0\phi_0 e_0}{h^2}, \quad (25)$$

which has a solution of the form

$$\hat{\xi}(z) = A e^{-ik_+ z} + B e^{-ik_- z} + C,$$

where k_{\pm} satisfies the dispersion relation

$$k_{\pm} = \frac{\omega/V_0 \pm i[(2\epsilon_0\phi_0^2/\rho\Delta h^3 V_0^2)(1 - 2T/\rho\Delta V_0^2) - 2\omega^2 T/\rho\Delta V_0^4]^{\frac{1}{2}}}{(1 - 2T/\rho\Delta V_0^2)}, \quad (26)$$

which is equivalent to Eq. (17) in the long wavelength limit ($kb \rightarrow 0$, $\frac{1}{2}k\Delta \rightarrow 0$). The boundary conditions

$$\hat{\xi}(0) = 0, \quad (27a)$$

$$\frac{d\hat{\xi}}{dt}(0) = i\omega\hat{\xi}(0) + V_0 \frac{\partial \hat{\xi}}{\partial z}(0) = 0, \quad (27b)$$

determine the displacement at the exit ($z = l$)

$$\hat{\xi}/e_0 = (Cl/4V_0\alpha^2)(1 + \gamma/\alpha^2)^{-1} \cdot [e^{-ik_+ l}(\cosh k_+ l + (ik_+/k_i) \sinh k_+ l) - 1], \quad (28)$$

and the velocity at the exit

$$\hat{v}/e_0 = (C/4\alpha^2)(1 + \gamma/\alpha^2)^{-1} \{2i\alpha \cdot [(\cosh k_+ l + (ik_+/k_i) \sinh k_+ l) e^{-ik_+ l} - 1] + e^{-ik_+ l} [(k_+^2 l/k_i) \sinh k_+ l + k_+ l \sinh k_+ l]\}, \quad (29)$$

where

$$C = 2\epsilon_0\phi_0 l(\rho\Delta h^2 V_0)^{-1}, \quad \gamma = \epsilon_0\phi_0 l^2(2\rho\Delta h^3 V_0^2)^{-1}, \\ \alpha = \omega l/2V_0.$$

B. A Simpler Approach

Problems of this sort are complicated by the interaction between the surface and the electric field perturbations. For the exciter, however, this restriction may be relaxed if the forces due to the perturbation of the shape of the surface are much smaller than the force set up by the change in the applied electric field. Under these conditions the force on the surface is independent of the surface perturbations, and the equation expressing conservation of momentum for a differential length of the jet may be written as

$$\int_0^{\rho\Delta z} d(\rho\Delta v_x) = \int_{-l/V_0}^0 \frac{2\epsilon_0\phi_0 e(t)}{h^2} dt. \quad (30)$$

For a sinusoidal signal voltage, the exit velocity is

$$\hat{v}_x/\hat{e} = C(\sin \alpha/\alpha) \exp(-i\alpha), \quad (31)$$

which is equivalent to the velocity obtained by taking the limit of Eq. (29) as $T \rightarrow 0$ and $\phi_0 \rightarrow 0$. Two features of this response deserve mention. The first is the existence of minima in the response at the frequencies $\alpha = n\pi$. At these frequencies, the jet passes through the entire length of the exciter in a time equal to an integral multiple of one cycle of the input signal. Since the force varies sinusoidally and the net velocity is approximately equal to the integral of the electric force over the time the jet spends in the exciter, the exit velocity is very small.

Also, the response falls off at higher frequencies because the integral of the force is very small after one period of the exciting voltage and the signal up to this time is "wasted." Thus, at higher frequencies the exciter, which is longer than a wavelength, is effectively shortened, and the magnitude of the response drops accordingly.

The velocity of the jet at the exit of the exciter as predicted by the approximate and the long wavelength approach is plotted in Fig. 6. At very low frequencies, growing waves exist inside the exciter which amplify the response to $(\sinh k_+ l)/k_+ l$ times its value when the waves were neglected. For higher frequencies, the waves no longer grow, and their effect is to shift the frequencies at which the maxima and minima of the response occur. In most physically realizable exciters, however, these effects are slight.

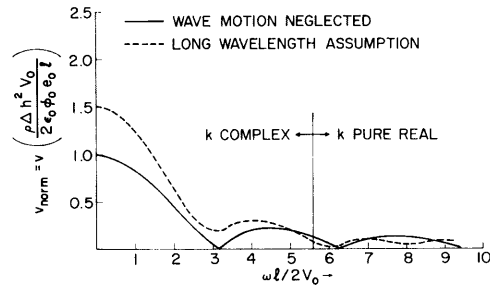


FIG. 6. Normalized transverse velocity of the jet at the exciter exit. ($\gamma = 0.695$.) The magnitude of the disturbance downstream of the exciter is determined primarily by this velocity.

C. A Nonuniform Field Exciter

We have seen that the parallel plate, planar exciter exhibits a series of minima in the frequency response. When the exciter is used experimentally to produce waves over a broad frequency range, these minima become objectionable, as they make it difficult to excite waves at some frequencies. In previous experiments, it has been noticed that the use of two spherical electrodes in place of the parallel plate electrodes resulted in a much smoother frequency response, probably because of the nonuniformity of the electric field. In order to analyze this situation theoretically, a new two-dimensional exciter model was studied. In this model, the parallel plate electrodes were replaced by two infinite cylinders, as shown in Fig. 7. Using the simpler model of the exciter as described in Sec. II B in which the surface tension and steady electric force are negligible, the equation of conservation of momentum can be applied to find an approximation to the velocity response of the jet.

To apply the equation, we must know the electric field at the surface of the jet, which can be determined by the solution of the electrostatic equations in the bicylindrical coordinate system⁵ defined by

$$x = \frac{a \sinh \eta}{\cosh \eta - \cos \theta}, \quad (32a)$$

$$z = \frac{a \sin \theta}{\cosh \eta - \cos \theta}, \quad (32b)$$

$$y = y. \quad (32c)$$

With the same conditions on the voltages and separations as in the planar exciter, the force per unit area as a function of the longitudinal position on the jet (θ) is

⁵ P. M. Morse and H. Feshbach, *Methods of Theoretical Physics* (McGraw-Hill Book Company, Inc., New York, 1953).

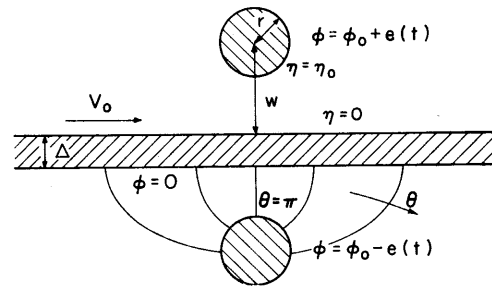


FIG. 7. The planar jet flowing through a nonuniform field exciter.

$$[2\epsilon_0(1 - \cos \theta)^2 \phi_0 e_0 e^{i\omega t}] / a^2 \eta_0^2.$$

In this expression, η_0 is the value of η which determines the position of the exciter electrode

$$\eta_0 = \cosh^{-1}(w/r),$$

where r is the radius of the cylindrical electrode, and w is the distance from its center to the surface of the jet. From the transformation equations

$$z = a \sin \theta / (1 - \cos \theta), \quad (33)$$

$$dz/dt = V_0, \quad (34)$$

and the equation of conservation of momentum, the velocity response is given as

$$\partial_z / e_0 = (\epsilon_0 \phi_0 / \rho \Delta a \eta_0^2 V_0) I(\omega a / V_0), \quad (35)$$

where

$$I(\alpha) = \int_0^{2\pi} (1 - \cos \theta) \cos [\alpha \sin \theta / (1 - \cos \theta)] d\theta.$$

A plot of $I(\alpha)$ versus α is shown in Fig. 8. This response curve does not exhibit the series of peaks and nulls characteristic of the parallel plate exciter but falls off steadily with increasing frequency, approaching zero asymptotically. The electric field associated with this exciter arrangement does not have any sharp changes or discontinuities in space, so that the jet in passing through the exciter sees a continuously changing field strength. From these

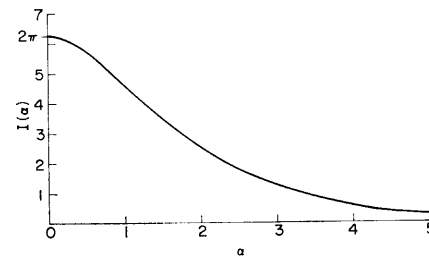


FIG. 8. Response of the nonuniform exciter, showing the normalized transverse velocity at the exit.

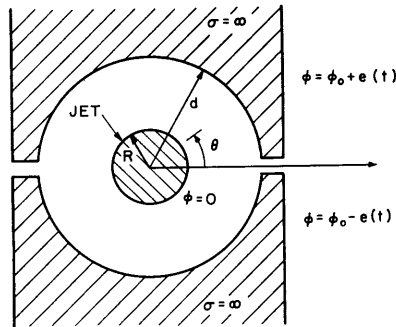


FIG. 9. The exciter for the circular jet in cross section.

results it might be inferred that a sharp discontinuity in the field is necessary to give peaks and nulls in the response curve, and a field which varies smoothly in space will give a response which falls off monotonically with frequency.

D. Excitation of Waves on a Circular Jet

So far we have been concerned exclusively with a two-dimensional planar jet. While a planar jet lends itself easily to theoretical analysis, it is extremely difficult to realize in the laboratory. A cylindrical jet, however, is easy to produce, and its theoretical analysis, while not so straightforward as that of the planar jet, is entirely possible. Just as we were concerned only with the antisymmetric mode in the discussion of the planar jet, we shall only consider those motions of the circular jet in which the cross section of the jet remains essentially unaltered, so that the jet moves uniformly in the direction transverse to the downstream direction (the mode $m = 1$).

The physical arrangement of the system is shown in Fig. 9. In the region downstream of the exciter, the outer electrode is at a constant potential, and the jet is grounded. In the exciter, the outer electrode is split into two semicircles, one at potential $\phi_0 + \phi_1$ and the other at potential $\phi_0 - \phi_1$. This difference in the two potentials leads to a force per unit length on the jet in the exciter region, which can be calculated using the Maxwell stress tensor. This procedure gives

$$F_{e1} = \frac{8\epsilon_0\phi_0\phi_1}{d(\ln d/R)(1 - R^2/d^2)}. \quad (36)$$

The force per unit length due to surface tension may be calculated by considering a short section of the circular jet displaced as a whole from its equilibrium position. The total equilibrium tension on the jet is given by the product of the surface tension and the length of the line on which it acts

and by a process similar to that used for a string under tension,

$$F_{t2} = 2\pi RT \partial^2 \xi / \partial z^2. \quad (37)$$

There will also be a force on the jet due to its displacement from equilibrium in the steady state electric field. This force has been calculated elsewhere in connection with electrical capacitors⁶ and is given as

$$F_{e2}/\xi = 2\pi\epsilon_0\phi_0^2(d^2 - R^2)^{-1}[\ln(d/R)]^{-2}. \quad (38)$$

With these forces, the equation of motion of the jet is

$$\pi R^2 \rho \left(\frac{\partial}{\partial t} + V_0 \frac{\partial}{\partial z} \right)^2 \xi = 2\pi RT \frac{\partial^2 \xi}{\partial z^2} + \frac{2\pi\epsilon_0\phi_0^2\xi}{(d^2 - R^2)(\ln d/R)^2} + \frac{8\epsilon_0\phi_0\phi_1}{d(\ln d/R)(1 - R^2/d^2)}, \quad (39)$$

and the exit displacement is

$$\xi/\phi_1 = (C_e l / 4V_0) \alpha^{-2} (1 + \gamma_e \alpha^{-2})^{-1} \cdot [e^{ik_r l} (\cosh k_i l + (ik_r/k_i) \sinh k_i l) - 1], \quad (40)$$

where

$$(\omega - kV_0)^2 = (2Tk^2/\rho R) - 2\epsilon_0\phi_0^2/(\rho R^2(d^2 - R^2)(\ln d/R)^2),$$

$$\gamma_e = \epsilon_0\phi_0^2 l^2 [2\rho R^2(d^2 - R^2)(\ln d/R)^2 V_0^2]^{-1},$$

$$C_e = 8\epsilon_0\phi_0 l [V_0 \rho \pi R^2 d (1 - R^2/d^2) \ln(d/R)]^{-1}.$$

Although this equation has been derived on an intuitive basis, it can be shown that in the long wavelength limit it is consistent with the previous exact result, Eq. (18). Except for multiplicative constants, it is the same result as the long-wave solution for the planar jet.

E. The Downstream Response of the Jet

The continuity of the displacement and slope at the exit of the exciter determines the disturbance downstream of the exciter, which satisfies Eq. (39) with the steady state voltage set equal to zero. By writing the downstream displacement in the form

$$\xi = [z(\xi'_0 + ik_r \xi_0)(k'z)^{-1} \sin k'z + \xi_0 \cos k'z] e^{-ik_r z}, \quad (41)$$

where ξ_0 is the exit displacement, ξ'_0 is the exit slope, and $k' = ik_i$ with $\phi_0 = 0$, we can see that it consists of two waves, one excited by the exit displacement and one by the exit velocity.

If k' is real, a stationary pattern of waves is set up on the jet. This pattern may be considered as

⁶ P. Moon and D. E. Spencer, *Field Theory for Engineers* (D. Van Nostrand, Inc., Princeton, New Jersey, 1961).

the superposition of two forward traveling waves, the slow wave with a propagation velocity slightly less than the jet velocity, and the fast wave with a propagation velocity slightly greater than the jet velocity. These two waves interact to give a wave pattern which is stationary in space, in much the same way as two waves with slightly differing frequencies interact to give the phenomenon of "beating" in time. If k' is imaginary, the fast and slow waves become decaying and growing waves. At some distance from the exciter the decaying wave becomes negligible, and the only disturbance on the jet is an exponentially growing wave. It is this wave which was studied to obtain measurements of the growth rate in Sec. I.

F. Experimental Results

Two types of measurements were made to test the theory of the exciter. The first was a measurement of the frequencies at which the minima in the response curve occur. To make these extremes evident, especially at the higher frequencies where the response of the exciter is small, an electric field large enough to cause growing waves was applied to the jet downstream of the exciter. The signal frequency was then adjusted until the disturbance reached a minimum and the frequency measured with an electronic counter. The results of this measurement are plotted in Fig. 10. The scatter around the theoretically predicted position of the minima may be partly attributed to the zero slope of the response curve at these points. From these data, we can conclude that the exciter does have the predicted minima in its response curve.

The response of the exciter as a function of frequency was also measured. Photographs of the jet were again taken with the aid of a strobachometer flashing at twice the frequency of the signal voltage. Measurements of the amplitude of the wave versus the distance along the jet were made from these photographs and the results plotted. These plots, one of which is shown in Fig. 11, indicate that the displacement response is sinusoidal in space, with the wavelength of the sinusoid decreasing as the frequency of the signal increases, as predicted by Eq. (41). From these plots the displacement response



FIG. 10. Frequency of the first three minima in the exciter response.

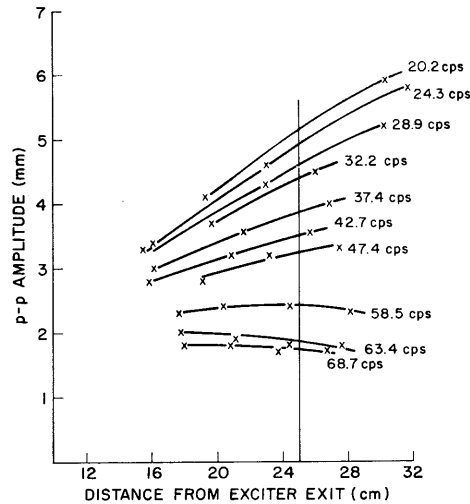


Fig. 11. Measurements of the amplitude of the displacement versus distance from the exciter exit for different frequencies, showing the effect of standing waves.

of the jet at any particular position may be found.

The values of the displacement were read from the graphs at a distance of 25 cm from the exciter, and these displacement values were plotted versus frequency to find the frequency response of the exciter. One of these plots, for the conditions

$$l = 1.4 \times 10^{-2} \text{ m}, \quad V_0 = 3.26 \text{ m/sec},$$

$$R = 1.59 \times 10^{-3} \text{ m}, \quad \rho = 10^3 \text{ kg/m}^3,$$

is shown in Fig. 12. Again, there is good agreement between the predictions of the theory and the experimental measurements.

ACKNOWLEDGMENTS

The author would like to thank Professor James R. Melcher for his helpful guidance during the course of the work.

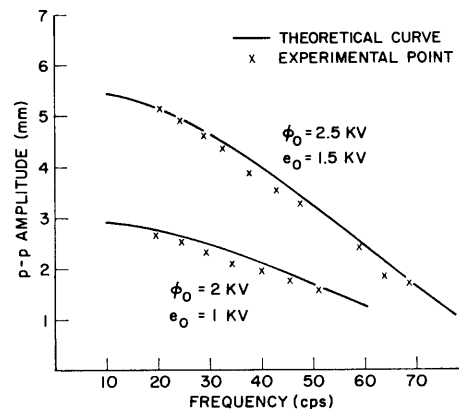


FIG. 12. Experimental and theoretical response of exciter, showing the displacement as a function of frequency.